

<b>REPORT DOCUMENTATION PAGE</b>					<i>Form Approved OMB No. 0704-0188</i>	
<small>The public reporting burden for this collection of information is estimated to average 1 hour per response, including the time for reviewing instructions, searching existing data sources, gathering and maintaining the data needed, and completing and reviewing the collection of information. Send comments regarding this burden estimate or any other aspect of this collection of information, including suggestions for reducing the burden, to Department of Defense, Washington Headquarters Services, Directorate for Information Operations and Reports (0704-0188), 1215 Jefferson Davis Highway, Suite 1204, Arlington, VA 22202-4302. Respondents should be aware that notwithstanding any other provision of law, no person shall be subject to any penalty for failing to comply with a collection of information if it does not display a currently valid OMB control number.</small>						
<b>PLEASE DO NOT RETURN YOUR FORM TO THE ABOVE ADDRESS.</b>						
<b>1. REPORT DATE (DD-MM-YYYY)</b>		<b>2. REPORT TYPE</b>			<b>3. DATES COVERED (From - To)</b>	
<b>4. TITLE AND SUBTITLE</b>				<b>5a. CONTRACT NUMBER</b>		
				<b>5b. GRANT NUMBER</b>		
				<b>5c. PROGRAM ELEMENT NUMBER</b>		
<b>6. AUTHOR(S)</b>				<b>5d. PROJECT NUMBER</b>		
				<b>5e. TASK NUMBER</b>		
				<b>5f. WORK UNIT NUMBER</b>		
<b>7. PERFORMING ORGANIZATION NAME(S) AND ADDRESS(ES)</b>					<b>8. PERFORMING ORGANIZATION REPORT NUMBER</b>	
<b>9. SPONSORING/MONITORING AGENCY NAME(S) AND ADDRESS(ES)</b>					<b>10. SPONSOR/MONITOR'S ACRONYM(S)</b>	
					<b>11. SPONSOR/MONITOR'S REPORT NUMBER(S)</b>	
<b>12. DISTRIBUTION/AVAILABILITY STATEMENT</b>						
<b>13. SUPPLEMENTARY NOTES</b>						
<b>14. ABSTRACT</b>						
<b>15. SUBJECT TERMS</b>						
<b>16. SECURITY CLASSIFICATION OF:</b>			<b>17. LIMITATION OF ABSTRACT</b>	<b>18. NUMBER OF PAGES</b>	<b>19a. NAME OF RESPONSIBLE PERSON</b>	
a. REPORT	b. ABSTRACT	c. THIS PAGE			<b>19b. TELEPHONE NUMBER (Include area code)</b>	

# Diamond Shaped Ring Laser Characterization, Package Design and Performance

Nancy Stoffel, Songsheng Tan, Charles Shick  
Infotonics Technology Center, 5450 Campus Drive, Canandaigua, NY 14424  
nancy.stoffel@infotonics.org

Wesley Bacon, Bryan Beaman  
Kodak Research Laboratory, 1999 Lake Avenue, Rochester, NY 14650

Alan Morrow, Malcolm Green  
Binoptics Corporation, 9 Brown Road, Ithaca, NY 14850  
amorrow@binoptics.com

Rebecca Bussjager, Steve Johns, Michael Hayduk, Joseph Osman, Reinhard Erdmann, Brian McKeon  
Air Force Research Laboratory SNRP, 25 Electronic Pkwy, Rome, NY 13441  
Rebecca.Bussjager@rl.af.mil

## Abstract

A semiconductor diamond-shaped ring laser was fabricated and packaged for further test and analysis as an element in digital photonic logic. The optical characteristics of the ring laser were quantified in order to design a prototype package. The mode field was found to be quasi-circular. Based on the mode field of the laser, coupling curves were calculated and Corning OptiFocus™ Lensed fiber was chosen to use for the four fiber outputs. Each fiber placement was actively optimized. Output power measurements were made for each facet before and after fiber coupling. Reflections from fiber tips were found to affect the final output power distribution of the device even though the fibers were anti-reflection (AR) coated, and additional effort was put into minimizing its variance. The packaged devices were tested for performance in digital photonic logic applications. Tests conducted to this point indicate that the packaging enabled a multiple port device of this type to be sufficiently portable for field testing.

## Introduction:

Digital Photonic Logic (DPL) is a candidate technology for advanced applications in digital networks such as ultra-fast all-optical switching, optical regeneration, and wavelength conversion as well as analog-to-digital conversion. Ring lasers are potentially useful because they propagate bi-directionally in the clockwise (CW) and counter-clockwise (CCW) directions<sup>1</sup> but can be forced into unidirectional propagation via laser injection, or by back reflection of the laser's own light via implantation of a mirror<sup>2</sup>. The bi-stable nature of the ring laser is exploited to create digital logic functions based on whether the signal propagates in the CW or CCW mode.

Initial work by BinOptics Corporation demonstrated design and fabrication capability for semiconductor ring lasers having properties of interest for DPL and analog to digital conversion applications. In a study funded by AFRL-Rome Research Site (Sensors Directorate), high speed characteristics of these lasers were investigated with promising results<sup>3</sup>. It is shown in this work that the bidirectional semiconductor ring laser could invert signals at a

rate of 12 Gb/s and that they could be switched with very small injected powers of 10μW. Care was required to match wavelength, polarization and injected pulse shape.

This paper describes a collaborative project designed to further the scientific study of ring lasers for DPL and other applications. Binoptics designed and simulated semiconductor diamond-shaped ring lasers with the objectives of demonstrating improved bi-stability, speed, and extinction ratios at high power. Infotonics developed a package providing a stable assembly for proper characterization of these devices and their properties. AFRL tested the final packaged devices for performance in DPL and other applications. Detailed in this paper is the process of designing, specifying, fabricating, integrating and some testing of components to provide a suitable package for the novel ring laser devices.

Optoelectronic packaging is an expensive, time-consuming operation requiring great precision in the placement and alignment of components. The package design and implementation affects the ultimate performance of the device significantly. The package was designed to maximize coupling to provide stability in position of the fibers relative to the device and to provide a stable operating environment, electrically and thermally. Prior to beginning the package design, several key parameters were measured; they included the far field profile of the ring laser beam, the light power and spectrum of the output, and coupling characteristics with lensed fibers. Four AR coated, polarization maintaining (PM), lensed fibers provide input/output ports for the diamond-shaped ring lasers. The fiber specifications and spacing were chosen based on coupling sensitivity measurements and a geometric analysis. In order to maximize the optical coupling between the device and the fibers, the fibers were aligned using active feedback and placed with submicron precision.

The prototype package design was constrained to modification of a prior optoelectronic package to reduce cost and wait time. Significant customization of the packages was required to meet the specific fiber connection requirements, and temperature control was required to control the output wavelength.

## Ring Laser Design

Semiconductor ring lasers were designed and fabricated by Binoptics, with the end facets formed by chemically assisted ion beam etching. The lasers, designed for operation at 1550 nm, propagated bi-directionally in either a cw or ccw direction, but could be forced into unidirectional propagation via laser injection. The round trip length is 500  $\mu\text{m}$  through 3.5  $\mu\text{m}$  wide ridge waveguides. Referring to Figure 1, there are two access ports at the top and bottom of the laser for input or output of light, with a 90° angle included for access to each of the facets at the access ports.

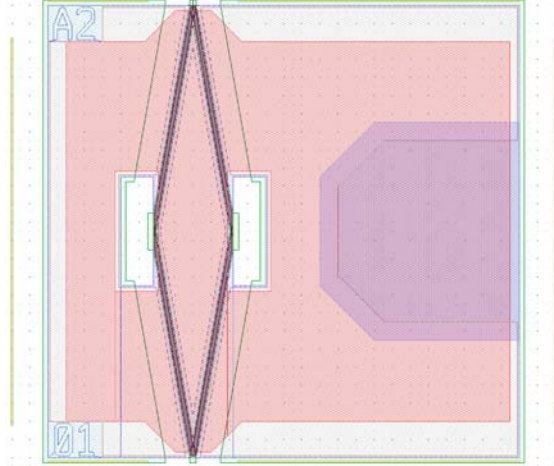


**Figure 1: Schematic of Ring Laser**

## Device Characterization for Package Design

The first step in the packaging design process was to profile the far field of the ring laser output beam. A BeamScan instrument profiled the beam size, uniformity and pointing angle. The head was placed in front of the ring laser with the detector position vertical to the right laser beam. The measured result is shown in Figure 2. The two dimensional laser beam profile in the right side of picture indicates that the power peak is off-center and shifted slightly towards the upper right side of the beam. This could be due to a slight deviation of the etched facet from 90°.

The inserted x and z power scan curves also show the non-symmetric nature of the power distribution. The widths ( $1/e^2$ ) of power curves at x and z are almost the same with an average of approximately 3.6 mm. Since the distance between the BeamScan head and the ring laser is approximately 20 mm, the divergent angle of the laser beam is approximately 10° in both directions. It indicates that the ring laser beam has a quasi-circular mode shape, which is similar to the mode shape of the coupling fiber. Compared with an elliptic mode shape of conventional Fabry Perot (FP) laser, the ring laser beam should have higher coupling efficiency with the optical fiber.

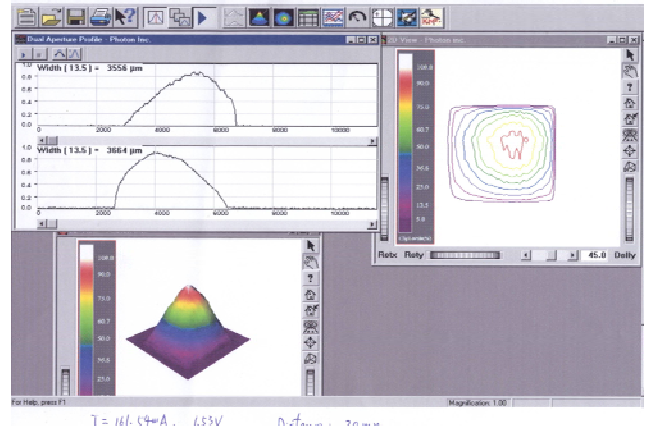


**Figure 2: Beam scan results of right beam of ring laser.**

## Fiber Coupling

There is mismatch of mode sizes between the ring laser waveguide and the single mode fiber, therefore a mode size transformation is necessary to improve the coupling efficiency. Although various micro lenses have been developed for the transformation of the mode size between laser diodes and single mode fiber, lensed fiber was utilized in this work. Figure 3 shows the normalized coupling efficiency with the beam waist of lensed fibers at the optimized coupling position calculated by the Kogelnik equation.<sup>4</sup>

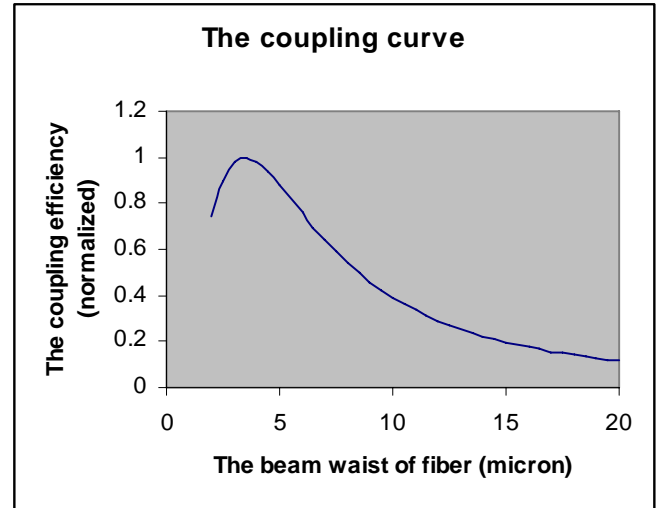


**Figure 3: A normalized coupling curve**

When the waist of the lensed fiber is equal to the mode size of ring laser waveguide, the highest coupling efficiency is obtained. The mode size of the ring laser beam is estimated to be between 3 and 4  $\mu\text{m}$  based on the width of the waveguide. Corning OptiFocus™ Lensed fiber was selected with a mode field of diameter of 3.3  $\mu\text{m}$  to optimize the coupling efficiency with the ring laser. Table 1 gives the specifications from the OptiFocus™ lensed fibers.<sup>5</sup>

**Table 1:** The specifications of Corning OptiFocus™ Lensed Fiber

OptiFocus™ Lensed fiber Specifications	Standard	Custom
MFD at Beam Waist ( $1/e^2$ @ 1550 nm)	$3.3 \mu\text{m} \pm 0.3 \mu\text{m}$	$> 3.0 \mu\text{m}$
Distance to Beam Waist	$> 20 \mu\text{m}$	Lens dependent
Far-field Divergence Angle $\theta_0$ (FWHM @ 1550 nm)	$20^\circ$	$< 20^\circ$
Fiber Type	SMF-28	SMF-28, PM, HI, others
Return Loss	$> 40 \text{ dB @ } 1550 \text{ nm}$	Lens dependent
*Coupling Efficiency per Pair	85%	Lens dependent

\* Measured by coupling light from one lensed fiber into the other.

A picture of the OptiFocus™ lensed fiber was acquired from Corning and was transferred to AutoCAD LT® in order to do a geometric analysis of the fiber placement. A major issue is the placement of two fibers in front of each side of the ring laser at the optimized coupling position without any geometric interference. Based on the design of the ring laser and diffraction effect of beams, these two lensed fibers should have included angle of  $90^\circ$ .

The analysis result is shown in Figure 4, where the AutoCAD drawing indicates the relative position when the lensed fiber tip is at the optimized coupling position of  $20 \mu\text{m}$  away from the ring laser facet. The clearance between the lensed fiber and the front side of the laser chip is approximately  $8.2 \mu\text{m}$  and the clearance between two lensed fibers is approximately  $16 \mu\text{m}$ . With the Newport laser welding system, those positioning tolerances on the lensed fiber placements can be held.

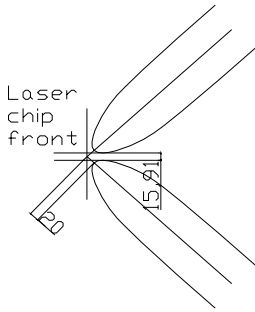


**Figure 4:** The geometric arrangement of two coupling lensed fibers.

A preliminary test was carried out to verify the above analysis. The ring laser used in this test was manufactured in an early batch with a higher threshold current,  $> 100 \text{ mA}$ . Two OptiFocus™ lensed fibers were mounted separately on micromanipulators. The test setup allowed each lensed fiber to be placed in the optimum coupling position with each one of ring laser beams. These two lensed fibers were connected to detectors of HP 8616 light power meter in order to monitor the coupling optical power levels.

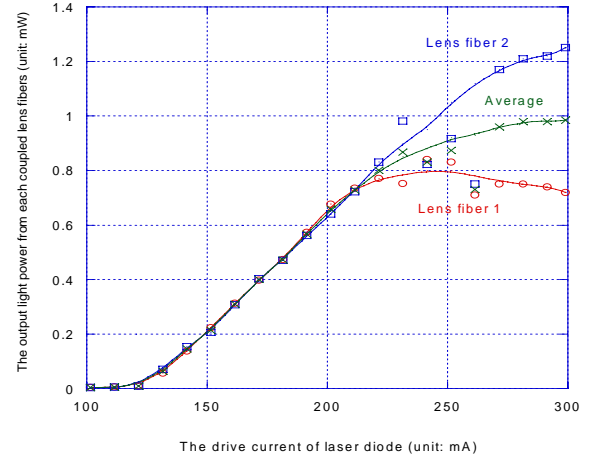


**Figure 5:** The optical power measured by the coupled fibers vs. the operating current of laser.

Figure 5 shows the measured photo intensity (PI) from each lensed fiber (measured simultaneously) vs. the operating current (I). For the current range from 100 to 210 mA, the light power levels from each lensed fiber were almost identical. When the laser diode current was over 210 mA, the power levels of the lensed fibers diverged from each other. The light power from lensed fiber 2 was approximately 1.2 mW at the diode drive current of 300 mA, while the light power from lensed fiber 1 was approximately 0.7 mW. This indicates the CW and CCW laser modes of the ring laser were not equal at the higher diode drive current.

### Packaging Architecture

A ring laser package was designed with four optical fiber connections. The fiber specifications and spacings were based on the measurements and analysis described in the previous section. Polarization maintaining fiber was chosen due to the device requirements. A thermoelectric cooler and thermistor were used to maintain the ring laser at  $25^\circ\text{C} \pm 0.1^\circ\text{C}$ . The maximum operating current of the ring laser was designed to be 300 mA.

Generally optoelectronic packages are made using gold plated Kovar because of its dimensional stability. The gold plating allows solder connections of subcomponents to the base and allows for hermetic sealing. The ring laser package requires a custom fabrication run due to its unusual requirements, making it somewhat costly with longer lead time. To minimize cost and delay, we chose to modify an existing package. Likewise an existing PC board was used to bring the electrical connections from the package wall feed-throughs to the laser. The placement of the components in the package needed to allow clearance for gripper tools used to move fibers during active alignment. In spite of the long wire bond lengths required, loop heights had to be kept low to keep the wires out of the path of the welding laser beam used to fasten the fibers in place.

The laser sub-mount was made narrow to allow the optical detector used in the pre-assembly characterization to get close enough to make accurate readings. This narrow base required precision assembly alignment to place the plane of the laser's four output beams coincident with the plane of the four optical fibers. The close fitting block beneath the submount (shown in yellow) was designed to help orient the submount and to serve as a heat spreader. The drawings of the final package design are shown in Figure 6a and 6b.

It was necessary to custom design a fixture for the Newport system laser welder to accommodate the ring laser design with its four coupled fibers.

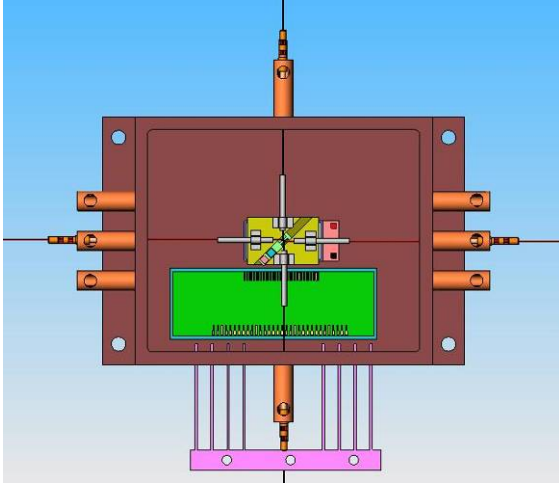


**Figure 6a:** Drawing of package design for ring laser.

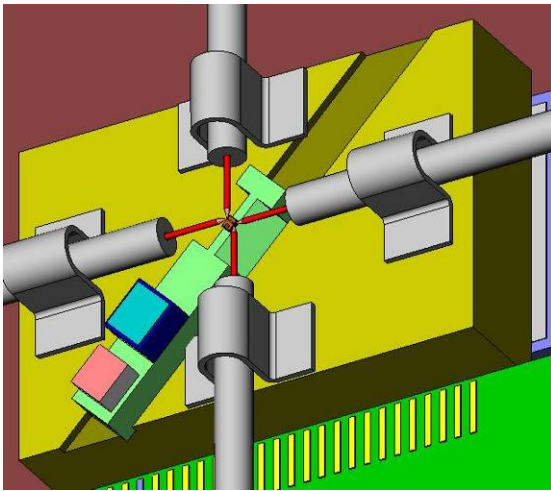
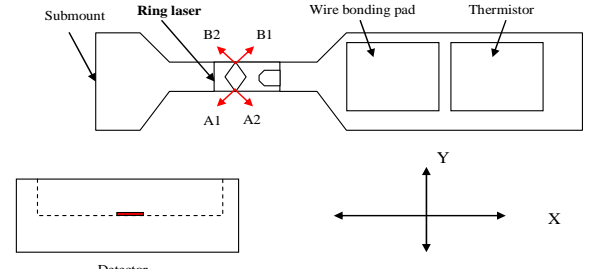


**Figure 6b:** Blown up view of laser mounted on submount with ferrulized fiber connections.

### Packaging Process and Results

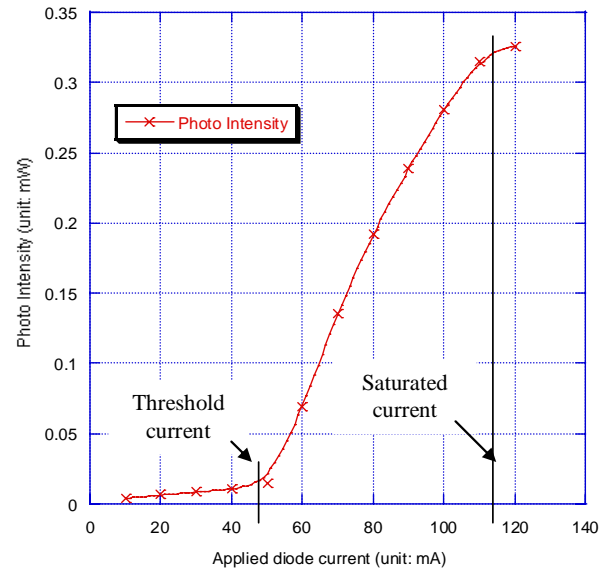
The ring chips were characterized after placement and solder bonding onto the submount. The measurements included the photointensity vs. applied diode current (PI-I) and uniformity determination of the beam intensity. This data was utilized to ensure that only the high quality laser diodes would be packaged. It also set a baseline of device performance for comparison after packaging.

Figure 7 is a schematic of the test with the ring laser on the submount, and the detector mounted on an X-Y movable stage.



**Figure 7:** Schematic of Test System

The forward current (I) was applied to the ring laser through probes. The detector was scanned along the X direction to collect the light beam. When the detector was moved as close as possible to the submount - where the Y coordinate was approximately 13 mm, only one broad peak was observed due to the overlap of two peaks.



**Figure 8:** The PI – I curve of the laser diode

A typical PI – I curve of the packaged ring laser diode is shown in Figure 8. It shows the threshold current and the saturated current of the laser diode. But the PI is only a relative value of the photo intensity, because the Y distance of 13 mm is too far for the detector to collect the whole beam intensity at one position.

When the detector was set at a greater distance from the submount such as  $Y = 25$  mm, two light peaks could be measured. The photo intensity ratio of these two beams can be measured ( $PI_{A1}/PI_{A2}$  or  $PI_{B1}/PI_{B2}$ ). (Note: Port labeling is shown in Figure 9.) After completing the A side measurement, the submount was rotated  $180^\circ$  in order to

measure the output of the B side facets. Measurements are compiled in Table 2 for a number of the submounts.

**Table 2:** Results of Characterization after mounting ring lasers on sub-mounts

Device #	Saturation Current	$PI_{A1}/PI_{A2}$	$PI_{B1}/PI_{B2}$
1	110 mA	1/1	1/1
3	120 mA	1/1	1/1
4	150 mA	1/4	1/2.5
5	160 mA	1/2	1/1.5
8	130 mA	1/2	1/2
9	170 mA	1/1	1/1.5
10	170 mA	1.5/1	1.5/1
12	140 mA	1/1	1/1.5
13	160 mA	1/1.5	1/1.5
14	180 mA	1/1	1/1
15	160 mA	1/1.5	1/1.5

After the process of mounting the ring laser to the submount, four of the fifteen lasers were non-functional and are not included in Table 2. Examination of the data in Table 2 shows a variation in the photo intensity of the beams. When the ratio of  $PI_{A1}/PI_{A2}$  is equal to 1, it indicates the intensities of the two beams were almost equal. When the ratio of  $PI_{A1}/PI_{A2}$  is equal to  $1/4$ , it indicates the intensity of the A2 beam is four times the intensity of the A1 beam. The detector is sufficiently far away from the facet of ring laser ( $> 25$  mm), so that the unequal intensity of these two beams is not caused by the reflection from the detector.

### Fiber Pigtail

The sub-mounts were placed in specially modified Kovar boxes, and fiber alignment was done utilizing a Newport 4200 fiber alignment system. During the fiber alignment, the laser diode was powered up to the saturation current ( $I_{sat}$ ) and the lensed fiber was connected to a detector to monitor the coupling light power. Once the fiber was placed in the optimal position, the fiber was fixed in place by using a laser to weld a clip in place to the fiber and to the package. The fiber alignment was done for each fiber individually. After a stabilization bake, the fiber ports were sealed with gold-tin solder. The whole fiber placement process of ring laser #15 was following the sequence of fiber coupling to facet A1, A2, B1, and B2. A Kovar lid with a glass window was placed on top of the box and sealed.

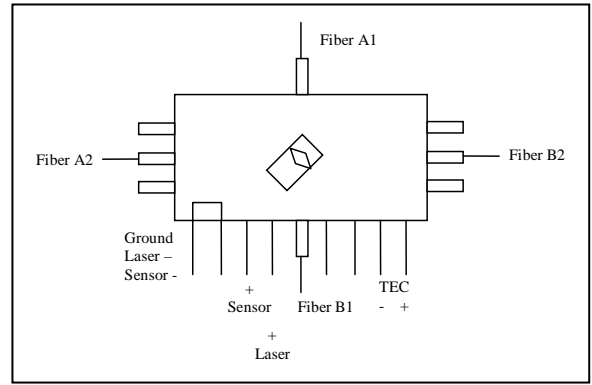


**Figure 9:** Diagram of package including fiber positions and electrical connections.

Table 3 contains the final test data for the packaged device ring laser #15. It lists the output light power and the return loss measurement from each fiber. The individual fiber positions and designations are shown in Figure 9. We were initially surprised that the final measured laser output was not the same as that recorded during the fiber placement operations, especially for the fiber A1 which was placed first. According to the submount test data, the beam intensity ratio of both sides of the device is almost equal (1:1.09). However in the packaged device, the beam intensity of the B side is much enhanced as compared to that of the A side (1:3.2), especially for fiber B2.

One possible explanation of this fact might involve residual reflections. There are two laser modes inside the ring laser: the CW mode and the CCW mode. The light output measured from fibers A1 and B1 is from the CW mode, and the output measured from fibers A2 and B2 is from the CCW mode. The return loss (RL) data indicates the highest return loss is from fiber A1. Although the light output from fiber A1 is from the CW laser mode, the higher reflections from fiber A1 back to the ring laser chip will enhance the CCW laser mode especially for fiber B2. This could explain the enhanced laser light output from fiber B2.

**Table 3:** Measurements of Packaged Ring Laser #15. Temperature was maintained at 25°C and  $I_{sat}$  of 160 mA.

Fiber Channel	A1	A2	B1	B2
Output	0.48 mW	0.57 mW	1.05 mW	2.33 mW
RL	- 28dB	- 43dB	- 31dB	- 42dB

Figure 10 is an infrared topography image of package #15. It shows the periphery of the laser chip, the trace of the ring laser waveguides, the two output facets, the two lateral reflection mirrors, and the four lensed fiber tips. The lensed fiber tip of A1 appears closer to the laser facet than the other



fibers. This is consistent with the higher measured RL of 28 dB from fiber A1.

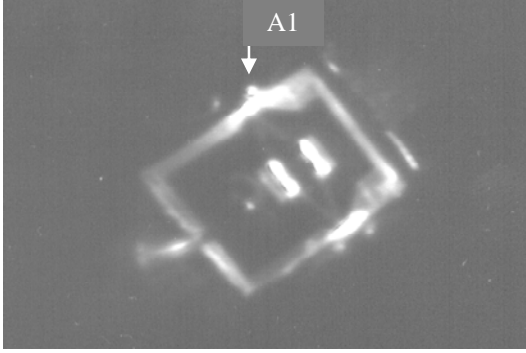


**Figure 10:** Infrared image of the ring laser #15

Although the real mechanism may be more complicated than this simple explanation of reflection from a fiber tip, it is important to be aware that these reflections can occur and will enhance the opposite laser mode. This factor is important for the successful packaging of ring lasers.

The infrared image also indicates that there may be significant leakage at the lateral mirror facets.

### Process Improvements

Subsequent to the packaging of the first device, ring laser #15, the process setup and methodology was altered in an effort to prevent the unbalanced output distribution observed. In order to solve this problem a change in the process methodology was required. The first fiber placement algorithm was the same as that used conventionally for FP lasers, but multiple detectors were incorporated to monitor the light output from all exit ports during the placement of the subsequent fibers. The newly placed fiber depended on not only its own light output, but also on the outputs of the previously placed fibers. Table 4 shows how the light outputs from the four lensed fibers packaged in this manner are more uniform.

**Table 4:** Measurements of Packaged Ring Laser Device # 13, assembled using additional detector feedback for sequential fiber placement. Temperature was maintained at 25°C and  $I_{sat}$  of 160 mA was measured.

Fiber Channel	A1	A2	B1	B2
Output	1.84 mW	1.70 mW	1.70 mW	1.72 mW

### Performance

Measured spectrum from port A2 of packaged ring laser #15 without injection is shown in Figure 11a for a current level of 0.060 A. Threshold current is 0.057 A. Even though the laser chip is cooled, the spectrum experiences a red shift with higher applied current levels shown in Figure 11b. Also the side modes increase in power with an increase in bias current.

When light is injected into the ring laser cavity and aligned with one of the ring cavity modes, the ring laser side modes become suppressed to a maximum of 35 dB. Figure

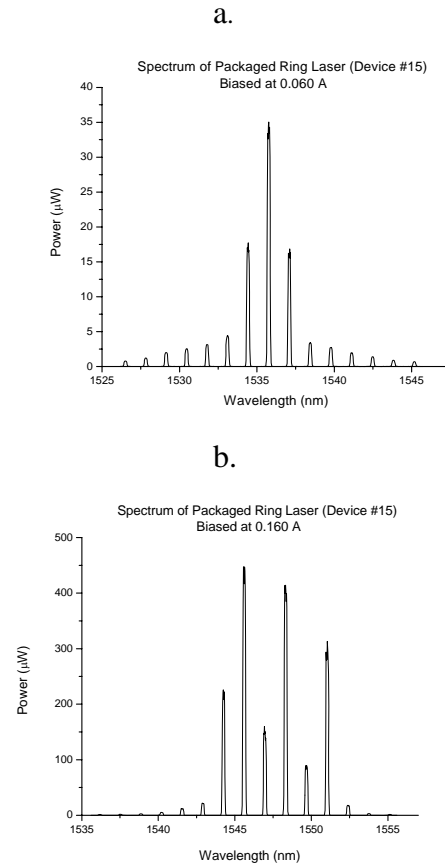
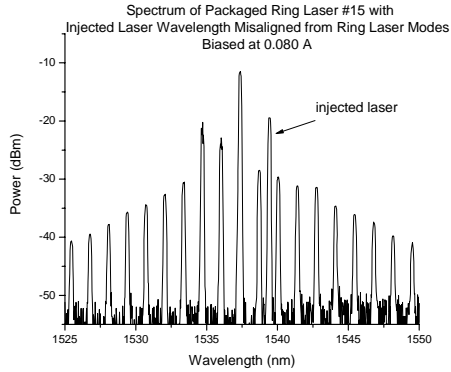


**Figure 11:** Optical spectrum of packaged ring laser # 15

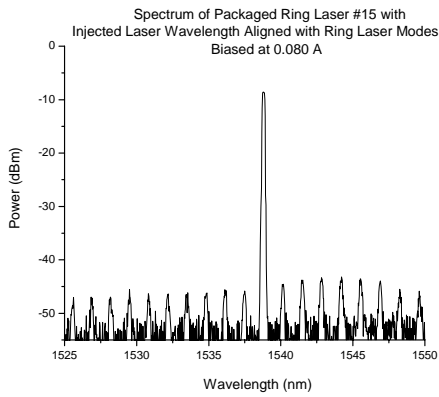
12a shows the spectrum when 1 mW (0 dBm) of light is injected into the cavity and not aligned to a resonance mode and 12b shows the side mode suppression when the injection is aligned with a resonance mode. Alignment does not have to be with the peak mode of the ring laser to force suppression. In figure 12b the laser experiences 34 dB side mode suppression when aligned with a side mode. When 10  $\mu$ W (-20 dBm) is injected suppression is reduced to approximately -30 dB. The combined injected light and ring laser mode experience some gain. In Figure 12a the peak mode amplitude is at -10 dBm, and it is roughly -8 dBm when the injection is tuned to a mode.

Optical injection of a modulated signal forces unidirectional propagation in the ring laser cavity. This is confirmed by observing two opposing outputs of the ring laser. Specifically, light was injected into port A1. An optical spectrum analyzer (OSA), Agilent 86142B, was connected to port A2 and monitored wavelength alignment. Port B2 co-propagated with the direction of A1 while Port B1 followed the opposing direction. The experimental setup is shown in Figure 13. A New Focus tunable laser, model 6300 Velocity, provided the injection. Its output was approximately 500  $\mu$ W. An erbium-doped amplifier (EDFA), Pritel Inc. LNHPFA-30, was used to provide more power to the JDSU Mach-Zehnder modulator, and a polarization controller provided the proper polarized state to the modulator. An Agilent signal generator, model 83650B, delivered the RF sinusoidal signal to the modulator, and a Krohn-Hite Corp. precision DC source, model 523, controlled the bias. The output from the modulator was connected to an in-line PM fiber power meter, Eigenlite PM 422. This power meter had a dialable attenuator

allowing the injected light power to be controlled and varied. The range of optical power was +10 dBm to -20 dBm corresponding to 10 mW to 10  $\mu$ W. Discovery Semiconductor 30S Lab Buddy detectors monitored the switching waveforms.



a.



b.

**Figure 12:** Optical Spectrum when laser injection wavelength is a) not aligned with ring laser modes, and b) aligned with a mode.

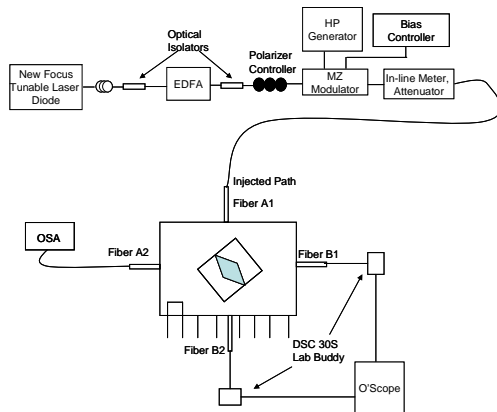


**Figure 13.** Experimental setup to characterize the packaged ring lasers.

Inversion of the waveform from port B2 compared with that from B1 was observed as the manifestation of the switching in propagation induced by the input optical signal. A sinusoidal signal was introduced in this case for test purposes. Switching was clearly observed up to 12 GHz, though the absolute limit was not determined at this time.

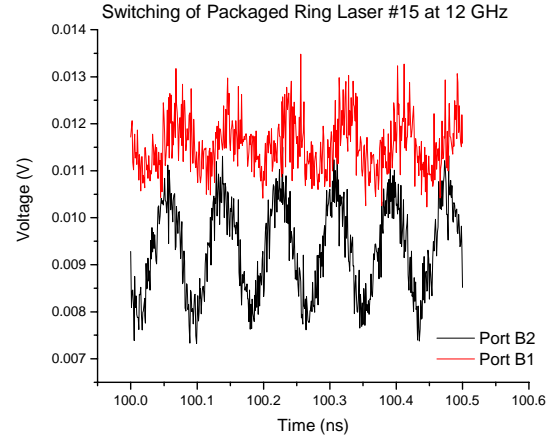


**Figure 14.** Sinusoidal switching at 12 GHz.

Figure 14 shows the results for 0 dBm injection, 0.2 V bias on the modulator, RF amplitude near 18 dBm, and ring laser operating at  $I_{sat}$ , 0.016 A. The two traces exhibit a phase shift of 16 ps between the two channels, which was due to a measured 50 mm difference in fiber lengths. The co-propagating signal is twice as large in amplitude, which can be attributed to the optical coupling of the fibers previously discussed, not to laser effects. The tests conducted to this point indicate that the packaging progress enabled a multiple port device of this type to be sufficiently portable for field testing. The actual digital application testing will require square as well as ultra-short mode-locked pulses; this will be reported in future work.

## Conclusions

Semiconductor diamond shaped ring lasers were fabricated, characterized and packaged to allow additional device testing and characterization. The ring lasers operated at the fiber window near 1550 nm and may offer a new approach to high speed switching for applications of digital photonic logic. Anti-reflection coated lensed fibers were coupled to each of the four facets. The output of each facet was measured before and after fiber coupling. It was found that the fiber placement affected the output distribution from the four ring laser facets, but modifications to the fiber coupling procedure minimized these differences.

## Acknowledgments

Infotonics Technology Center and Binoptics Inc. acknowledge support for this work through AFRL Grant Award F30602-03-2-0228.



## References

---

<sup>1</sup> United States Patent No. 5,132,983, “Optical Logic Using Semiconductor Ring Lasers”

<sup>2</sup> United States Patent No. 5,764,681, “Directional Control Method and Apparatus for Ring Laser”

<sup>3</sup> Final report to Air Force Research Lab in Rome, NY, “Optical Injection and Switching using Diamond Shaped Semiconductor Ring Lasers for Analog to Digital Photonic Converters”, Contract F30602-03-C-0220.

<sup>4</sup> H.Kogelnik, Bell. Syst. Tech. J., 48, 2909 (1969).

<sup>5</sup> Corning OptiFocus™ Lensed Taper Product Information , P1102, Issued October 2005.

[www.corning.com/photonicmaterials/products\\_services/optifocus](http://www.corning.com/photonicmaterials/products_services/optifocus)